



Contents lists available at ScienceDirect

Chemical Engineering Journal

journal homepage: www.elsevier.com/locate/cej

Integration of catalytic wet peroxidation and membrane distillation processes for olive mill wastewater treatment and water recovery

Bruno M. Esteves^{a,b}, Rita Fernandes^{b,c}, Sergio Morales-Torres^d,
Francisco J. Maldonado-Hódar^d, Adrián M.T. Silva^{b,c,*}, Luis M. Madeira^{a,b,*}

^a LEPAE – Laboratory for Process Engineering, Environment, Biotechnology and Energy, Faculty of Engineering, University of Porto, Rua Dr. Roberto Frias, 4200-465 Porto, Portugal

^b ALiCE - Associate Laboratory in Chemical Engineering, Faculty of Engineering, University of Porto, Rua Dr. Roberto Frias, 4200-465 Porto, Portugal

^c Laboratory of Separation and Reaction Engineering - Laboratory of Catalysis and Materials (LSRE-LCM), Faculty of Engineering, University of Porto, Rua Dr. Roberto Frias, 4200-465 Porto, Portugal

^d NanoTech – Nanomaterials and Sustainable Chemical Technologies, Department of Inorganic Chemistry, Faculty of Sciences, University of Granada, Avda. Fuente Nueva, 18071 Granada, Spain

ARTICLE INFO

Keywords:

Fenton
Heterogeneous
Catalyst
DCMD
Fixed-bed reactor
OMW

ABSTRACT

The degradation of organic matter present in olive mill wastewater (OMW) and the recovery of water were studied by the integration of catalytic wet peroxidation (CWPO) and direct contact membrane distillation (DCMD) for the first time. The oxidation step was performed in a fixed-bed reactor (FBR) working in continuous mode ($\text{pH}_0 = 4.0 \pm 0.2$, 60°C , $Q = 0.75\text{ mL/min}$, $[\text{H}_2\text{O}_2]/[\text{COD}]_{\text{feed}} = 2.3 \pm 0.1\text{ g H}_2\text{O}_2/\text{g O}_2$). Samples of OMW diluted by 5- and 7.5-fold were used (OMW-5 \times and OMW-7.5 \times , respectively), corresponding to inlet chemical oxygen demand (COD) values of 3562 ± 68 and $2335 \pm 54\text{ mg/L}$, total phenolic content (TPh) of 177 ± 17 and $143 \pm 7\text{ mg GA}_{\text{eq}}/\text{L}$, and total organic carbon (TOC) of 1258 ± 63 and $842 \pm 45\text{ mg/L}$, respectively. The FBR was loaded with 2.0 g of a Fe-activated carbon derived-catalyst, prepared by using olive stones as the precursor, in line with a circular economy model approach. The catalyst was selected based on the activity and stability towards polyphenolic synthetic solutions shown in previous works of the team, while actual OMW samples were used in this work. CWPO-treated samples of OMW allowed the operation of the DCMD unit at higher fluxes than with the analogous untreated ones, also showing higher rejections of organic matter from the feed solution upon DCMD, highlighting the beneficial effect of this novel configuration. Using a pre-treated sample of OMW-7.5 \times as feed solution ($Q = 100\text{ mL/min}$, $T_{\text{permeate}} \approx 18^\circ\text{C}$, $T_{\text{feed}} \approx 66^\circ\text{C}$), the produced permeate water stream presented several parameters well-below the legislated thresholds required for direct discharge for crops irrigation, including total suspended solids ($\text{TSS} < 10\text{ mg/L}$), TPh ($< 0.01\text{ mg GA}_{\text{eq}}/\text{L}$), biochemical oxygen demand ($\text{BOD}_5 < 40\text{ mg/L}$), and dissolved Fe ($< 0.06\text{ mg/L}$). Moreover, the resulting concentrated OMW-retentate streams could be recirculated to the FBR and maintain the same removal efficiencies obtained previously, despite the increased initial organic loadings of the retentate after DCMD.

List of Acronyms and Abbreviations

AOP	Advanced oxidation process
APHA	American Public Health Association
BOD ₅	Biochemical oxygen demand (5-days)
COD	Chemical oxygen demand
CWPO	Catalytic wet peroxide oxidation
DCMD	Direct contact membrane distillation
DW	Distilled water

(continued on next column)

(continued)

List of Acronyms and Abbreviations

EDX	Energy dispersive X-ray
FAOSTAT	Food and Agriculture Organization Corporate Statistical Database
FBR	Fixed-bed reactor
GA _{eq}	Gallic acid equivalent
LEP	Liquid entry pressure
OMW	Olive mill wastewater

(continued on next page)

* Corresponding authors at: ALiCE - Associate Laboratory in Chemical Engineering, Faculty of Engineering, University of Porto, Rua Dr. Roberto Frias, 4200-465 Porto, Portugal.

E-mail addresses: adrian@fe.up.pt (A.M.T. Silva), mmadeira@fe.up.pt (L.M. Madeira).

<https://doi.org/10.1016/j.cej.2022.137586>

Received 6 March 2022; Received in revised form 11 June 2022; Accepted 14 June 2022

Available online 16 June 2022

1385-8947/© 2022 The Authors. Published by Elsevier B.V. This is an open access article under the CC BY-NC-ND license (<http://creativecommons.org/licenses/by-nc-nd/4.0/>).

(continued)

List of Acronyms and Abbreviations	
OSAC	Olive stone-derived activated carbon
PTFE	Polytetrafluoroethylene
TDS	Total dissolved solids
TEM	Transmission electron microscopy
TSS	Total suspended solids
TOC	Total organic carbon
TPh	Total phenolic content
List of Variables	
β	Concentration factor, -
ΔP	Transmembrane pressure (kPa)
A	Effective membrane area (m ²)
$C_{\text{feed},0}$	Initial concentration in the feed (mg/L)
C_{permeate}	Permeate concentration (mg/L)
$C_{\text{retentate}}$	Retentate concentration (mg/L)
J	Permeate flux (kg/m ² •h)
Q	Volumetric flowrate (mL/min)
R	Rejection (%)
S_{BET}	BET surface area (m ² /g)
t	Time (h)
V_{meso}	Volume of mesopores (cm ³ /g)
W	Mass of distillate (kg)
W_{cat}	Mass of catalyst (g)
W_0	Volume of micropores (cm ³ /g)

1. Introduction

The pollution of water sources, intensified by industrialization, fast urbanization, and climate changes, is a rising global crisis that threatens humans, wildlife, and environmental health. Agricultural and industrial activities are the main sources of water consumption and pollution on a global scale. The food processing industry is among the largest water-consuming activities per ton of product processed, with tap and groundwater representing a major fraction of its needs, which almost always entails financial costs to obtain and/or to purify [1,2].

According to FAOSTAT (Food and Agriculture Organization Corporate Statistical Database) data on crops around the world, the water footprint of the olive oil processing industry (i.e., the sum of water used in all steps and unit operations required for extraction of olive oil) can be as high as 14 500 m³ per ton of oil extracted [3,4]. Despite the seasonal production, wastewaters generated by olive mills – known as olive mill wastewater (OMW) – can represent upwards of 50% relative to the total water inputs in such agroindustry sector, depending on the extraction process employed [3,5]. The high organic load of OMW – including several phenols, organic acids, tannins, pectins, among other organic and inorganic compounds – along with its acidic pH, low biodegradability and high solids content, are known to cause severe environmental harm to water bodies [6]. In particular, the high phenolic content of OMW is responsible for its phytotoxic properties and antimicrobial behavior, also known to cause distress in wastewater treatment plants operating with conventional biological units. Moreover, the high variability in its composition – related to numerous factors such as weather, cultivation practices, and/or extraction process – makes the adoption of a centralized treatment solution a historically complex problem to solve [7,8].

As water becomes scarcer, it is vital to prioritize wastewater treatment and reuse to maintain the sustainability of natural and urban water cycles [9]. In this work, we evaluate for the first time the integration of an advanced oxidation technology for OMW treatment – the heterogeneous Fenton-like oxidation, also known as catalytic wet peroxide oxidation (CWPO) – with a downstream membrane separation process for water recovery – the direct contact membrane distillation (DCMD) technology.

In the first step, the oxidation potential of the highly reactive and non-selective hydroxyl radicals (HO•) – generated from the catalytic decomposition of H₂O₂ in the presence of ferrous ions in an acidic medium [10] – is explored for the depuration of OMW. In this stage, the process implementation can benefit from the naturally-low pH of OMW to help reduce costs associated with chemicals for wastewater acidification required for optimum CWPO operation. Additionally, Fe-supported catalysts are known to tackle the generation of the iron-rich sludge characteristic of the homogeneous process, thus also eliminating its downstream handling costs [11,12]. For this purpose, the most recent work of the team [13,14] has been dedicated to the development and detailed characterization of tailored Fenton-like catalysts synthesized from solid by-products of the olive oil industry (namely olive stones), and thus, ultimately, to the adoption of an environmental circular economy model within this industry.

Membrane distillation is a thermally-driven separation technology widely adopted in desalination, but also for different environmental applications related to water/wastewater treatment [15]. A membrane module, operated at non-isothermal conditions between both sides of a microporous hydrophobic membrane, generates a transmembrane vapor pressure difference (ΔP) between the permeate (cold) and retentate (hot) sides that allows water vapor (or volatile compounds) to selectively pass the membrane pores, preventing the mass transfer of the liquid [16]. When compared to other separation technologies, membrane distillation processes are operated at a lower temperature than conventional distillation, also involving the generation of lower hydrostatic pressures than nanofiltration or reverse osmosis, for example [15,17].

It has been proved that direct contact membrane distillation (DCMD) is an efficient process for wastewater treatment, either as a method to produce a less environmentally-hazardous stream of permeate and/or to concentrate and recover valuable compounds [18–20]. Thus, aiming at the recovery and reuse of water (e.g., for crops irrigation or machinery washing activities), the second step of the proposed process herein envisaged comprises the use of a DCMD unit. Among the possible configurations, DCMD was selected for its simplicity of operation, as the condensation step occurs inside the membrane module.

Reports considering an advanced oxidation process (AOP) as an alternative DCMD pre-treatment of OMW were not found in the literature. Therefore, Table 1 only summarizes the main findings with the membrane distillation technology (without AOPs) for OMW treatment/valorization [20–25]. As highlighted therein, the few reports available mainly report the recovery/concentration of polyphenols rather than OMW depuration and production of water for reuse. For instance, the work of El-Abbassi *et al.* [21,22] focused on the operation of a DCMD unit alone, testing membranes with distinct properties and tuning the operational conditions to maximize polyphenols concentration in the retentate stream. However, the higher flux decline caused by membrane fouling/scaling when operating highly-loaded effluents poses a significant process limitation. The authors later explored two pre-treatment processes – coagulation/flocculation and microfiltration – and their effect on the separation efficiency. In particular, microfiltration was defined as the best pre-treatment process to remove suspended solids from OMW (30% vs. 23% with coagulation/flocculation), and enhance the initial permeate flux in DCMD ($J_0 = 7.7, 6.9, \text{ and } 5.6 \text{ L/h m}^2$ for microfiltration-treated, coagulation/flocculation-treated, and raw OMW, respectively [23]).

Up to the authors' knowledge, the application of an integrated

Table 1

Literature survey of membrane technology applied for the treatment and/or valorization of OMW with indication of membrane characteristics, operational conditions, and achieved standards.

Process scheme	Membrane Characteristics	MD operational conditions	Achieved Standards	Ref.
DCMD	Capillary membrane of polypropylene	$T_{\text{feed}} = 30\text{--}50\text{ }^{\circ}\text{C}$ $T_{\text{perm}} = 15\text{ }^{\circ}\text{C}$ (H_2O) $A = 30\text{ cm}^2$ $Q_{\text{feed}} = 70\text{ L/h}$ $Q_{\text{perm}} = 60\text{ L/h}$ $[\text{TPh}]_{\text{feed}} = 2500\text{ ppm}$	$J_{\text{average}} = 1.1\text{--}6.5\text{ kg/h m}^2$ $[\text{TPh}]_{\text{permeate}} = 3.0\text{--}3.3\text{ ppm}$ $[\text{TOC}]_{\text{permeate}} = 450\text{--}615\text{ mg/L}$ (depending on the feed temperature values)	[20]
Vacuum Membrane Distillation	Capillary membrane of polypropylene	$T_{\text{feed}} = 50\text{ }^{\circ}\text{C}$ $A = 30\text{ cm}^2$ $Q_{\text{feed}} = 70\text{ L/h}$ Vacuum = 5 mbar $[\text{TPh}]_{\text{feed}} = 150\text{--}2500\text{ ppm}$	$J_{\text{average}} = 19\text{ kg/h m}^2$ (at TPh of 2500 ppm) $[\text{TPh}]_{\text{permeate}} = 4.4\text{--}10\text{ ppm}$ (depending on initial concentration)	[20]
DCMD	Two commercial membranes tested: PTFE and Polyvinylidene fluoride	$T_{\text{feed}} = 40\text{ }^{\circ}\text{C}$ $T_{\text{perm}} = 20\text{ }^{\circ}\text{C}$ (H_2O) $t = 9\text{ h}$ Stirring rate = 500 rpm	PTFE membrane with higher separation coefficient (α) for polyphenols (99%) than polyvinylidene fluoride membrane (89%) α values for TPh close to 100% after 8 h independently of the membrane used; higher J values for the membrane with higher pore size	[21]
DCMD	Three commercial PFTE membranes with distinct mean pore sizes	$T_{\text{feed}} = 40\text{ }^{\circ}\text{C}$ $T_{\text{perm}} = 20\text{ }^{\circ}\text{C}$ (H_2O) $t = 8\text{ h}$ $A = 2.75 \times 10^{-3}\text{ m}^2$ Stirring rate = 500 rpm	$J_0 = 7.9\text{ vs. }6.9\text{ L/h m}^2$ for microfiltration vs. coagulation/flocculation pre-treatment; Concentration factor (β) ranged from 1.56 to 2.93, depending on the phenolic compound	[22]
Coagulation/flocculation → DCMD & Microfiltration → DCMD	PFTE flat-sheet membrane	$T_{\text{feed}} = 40\text{ }^{\circ}\text{C}$ $T_{\text{perm}} = 20\text{ }^{\circ}\text{C}$ (H_2O) $t = 40\text{ h}$ $A = 2.75 \times 10^{-3}\text{ m}^2$ Stirring rate = 500 rpm	91% TSS and 26% TOC reductions after the microfiltration step; 63% TOC reduction after nanofiltration; J of ca. 8 L/h m ² after 360 min for Vacuum Membrane Distillation	[23]
Microfiltration → Nanofiltration → Vacuum Membrane Distillation	Flat-sheet membrane of Polyvinylidene fluoride	$T_{\text{feed}} = 30\text{ }^{\circ}\text{C}$ $A = 55\text{ cm}^2$ Vacuum = 30 mbar $Q = 180\text{ L/h}$	35% flux decrease after	[24]
Microfiltration → DCMD	Flat-sheet Polyvinylidene fluoride	$T_{\text{feed}} = 40\text{ }^{\circ}\text{C}$ $T_{\text{perm}} = 10\text{ }^{\circ}\text{C}$ (H_2O)		[25]

Table 1 (continued)

Process scheme	Membrane Characteristics	MD operational conditions	Achieved Standards	Ref.
		$A = 40\text{ cm}^2$ $Q_{\text{feed}} = 150\text{ L/h}$ $Q_{\text{perm}} = 80\text{ L/h}$	ca. 7 h (4.8 to 3.0 kg/h m ²)	

process comprising heterogeneous Fenton-like oxidation followed by a DCMD separation for OMW treatment and water recovery has never been addressed in the literature as an integrated solution for the management of residues within this agro-industry. The present CWPO-DCMD integrated solution presents a novel approach with several advantages for OMW management, including:

- A pre-treatment step based on an oxidation reaction rather than a physical and/or chemical separation process;
- Repurpose of a solid by-product as catalyst support, thus handling both sources of waste (solid and liquid) from this agro-industry in the same treatment scheme;
- The potential to reduce membrane fouling – and therefore to improve permeate fluxes – via the dissolution of organic matter triggered by the oxidation step;
- The theoretical elimination of dissolved Fe in the treated water stream (often observed when operating with CWPO alone), since the potential leaching of iron from the solid catalyst would be kept in the retentate side of the DCMD unit (and eventually recirculated to the fixed-bed reactor (FBR));
- Improvement of the quality and quantity of reclaimed water produced upon the integration of both units in a continuously operating system when compared to stand-alone processes.

Therefore, this study aims to explore the aforementioned advantages of both processes to: (1) reduce OMW organic load, as inferred by its total phenolic content (TPh), chemical oxygen demand (COD), and total organic carbon (TOC); (2) ensure the continuous production of a stream of treated OMW by using an in-house synthesized catalyst in a fixed-bed reactor to operate continuously and feed the DCMD unit; (3) recover and characterize treated water (permeate) to check compliance with legislated standards for direct discharge or irrigation purposes; and (4) evaluate the possibility of recirculating the produced concentrated stream of OMW back to the FBR unit.

This work provides a circular economy model for this sector that emphasizes the “waste-to-value” approach, aligned with the most recent EU regulation [26] that foresees a wider use of reclaimed water for agricultural irrigation. The regulation, addressing the minimum pre-conditions for water reuse, is set to be enforced as early as 2023 due to the increasing pressure on water resources caused by urban development and agriculture, leading to water scarcity and water quality deterioration across all EU member states.

2. Materials and methods

2.1. Catalyst and olive mill wastewater

The catalyst used in the FBR runs was prepared via incipient wetness impregnation using $\text{Fe}(\text{NO}_3)_3 \cdot 9\text{H}_2\text{O}$ (Merck) as the iron precursor, to a theoretical load of 5 wt% of Fe. The selected Fe-load was determined based on a compromise between the adsorptive and catalytic behaviours of the resulting catalyst. While a decrease in effective Fe-loading may hamper the catalytic efficiency of the process, an excessive amount of iron can also result in a similar outcome. With a higher Fe/activated carbon ratio, two detrimental outcomes were commonly observed: blockage of porosity (and therefore accessibility of contaminants and

H₂O₂ to Fe active-sites inside the porous structure of the material), and agglomeration of Fe–nanoparticles into big clusters that present smaller surface/contact area in comparison to smaller and more homogeneously distributed ones [14,27].

The active iron phase was anchored to an olive stone derived-activated carbon support (OSAC), previously synthesized by sequential carbonization (N₂ atmosphere) and activation (CO₂ atmosphere) in a horizontal tube furnace at 800 °C, as schematically represented in Fig. 1. After impregnation, the resulting material was subject to thermal treatment (350 °C in N₂) to decompose the iron salt and produce the catalyst [13,14].

In brief, the resulting catalyst (OSAC-Fe) is a microporous material ($W_0 = 0.24 \text{ cm}^3/\text{g}$) with some contribution of mesopores ($V_{\text{meso}} = 0.05 \text{ cm}^3/\text{g}$) in the structure, presenting a well-developed surface area ($S_{\text{BET}} = 588 \text{ m}^2/\text{g}$). Small circular ($d_{\text{XRD}} < 4 \text{ nm}$) and well-dispersed iron nanoparticles at the catalyst surface (observed by transmission electron microscopy, TEM, and energy dispersive X-ray spectroscopy, EDX – Fig. 2) were predominantly identified by X-ray diffraction as α -Fe₂O₃ (α -hematite).

The OMW used in this study was obtained from the 3-phase decanter's exit of a small-size olive mill from the northern region of Portugal during the 2019 campaign. Imhoff cones were used to separate particulate and settleable suspended matter (24 h of settling time), and the supernatant was collected for physicochemical characterization (Table 2). Samples were then divided into several 1 L containers and frozen (-15 °C) until required for the experimental runs. The initial organic load of the effluent was adjusted by dilution with distilled water; the effluent supernatant was diluted by 5-fold and 7.5-fold to recreate the potential biological stabilization and/or rain dilution occurring in a scenario where the effluent would be stored in an open-air pond [28].

2.2. Fixed-bed reactor set-up: CWPO experiments

Catalytic runs were performed in an up-flow jacketed fixed-bed reactor (borosilicate glass column) with inner dimensions of $H = 12 \text{ cm}$ and $D = 1.5 \text{ cm}$. The catalyst ($W_{\text{cat}} = 2.0 \text{ g}$ and particle size fraction of 0.45–0.80 mm – corresponding to approximately 2/3 of the reactor's height) was placed at the center of the column; 1 mm diameter inert glass spheres were used to fill the remaining void spaces and both ends were capped with glass wool to prevent clogging of the inlet and outlet tubing – cf. Fig. 3. The FBR was connected to a recirculating thermostatic bath (VWR, mod. 89202–912), and the temperature was set to 60 °C. The feed solution (OMW) was placed into a 3-neck round bottom flask (500 mL), agitated at 300 rpm, and heated to 60 °C using a magnetic stirrer with a hot plate (Falc Instruments). To guarantee an equitable comparison between runs, pH values were maintained at 4.0 ± 0.2 (i.e., the initial pH of sample OMW-5 \times) – adjustments to slightly acidify the OMW-7.5 \times sample were performed using H₂SO₄ 1.0 M. As illustrated in Fig. 3, the flask was connected to a reflux condenser at 15 °C (to avoid evaporation of the feed OMW), the solution's pH and temperature were continuously measured by a WTW Inolab pH-meter (mod. Level 2P), and

fed to the reactor by a peristaltic pump (NEW–ERA, mod. NE–900).

In a typical run, the column was initially filled with distilled water, the system was allowed to reach the desired temperature, and then the H₂O₂ (30% w/v, VWR) was added to the feed flask and fed to the FBR (initial instant of the oxidation experiments, $t = 0$). The oxidative behavior of the H₂O₂ in the feed vial was checked over time, and the maximum removals observed were <4% for TOC, <6% for COD, and <10% for TPh (results not shown for brevity). As detailed in a previous work of the team [14], the required amount of H₂O₂ is dependent on the solution's initial COD, which was kept at a fixed feed [H₂O₂]/[COD] ratio of $2.3 \pm 0.1 \text{ g H}_2\text{O}_2/\text{g O}_2$; this ratio was set as to maximize oxidation efficiencies and reduce the amount of unreacted oxidant at the reactor's outlet. The determined ratio is in the same range as the one proposed by other authors assuming the theoretical complete oxidation of COD [29]. In each run, the system was operated continuously for 20 h at a volumetric flow rate (Q) of 0.75 mL/min, requiring the addition of untreated OMW to the feed flask approximately every 10 h (i.e., once every run). The operational conditions of the FBR unit were established following the results of a previous work of the team [14], and as suggested therein, the contact time (W_{cat}/Q) was increased by 2-fold to $W_{\text{cat}}/Q = 2.66 \text{ g min/mL}$; under such conditions, the performance of the catalyst bed was improved and maintained stable for $\approx 40 \text{ h}$ of operation, and thus it was not substituted for this set of experiments (although a washing procedure with distilled H₂O was performed upon changing the initial effluent loading). Samples of the resulting CWPO-treated effluent were then discontinuously forwarded to the DCMD unit.

2.3. DCMD experimental set-up

DCMD experiments were performed in a laboratory set-up similar to that described in a previous study [30]. A polytetrafluoroethylene (PTFE) membrane (0.22 μm pore size, 150 μm thickness) from Merck Millipore (FGLP Fluoropore®) was selected for the DCMD unit, based on several reviews [15,31,32] that highlight its efficiency for membrane distillation and good properties related to pore size distribution, hydrophobicity, chemical resistance, and thermal stability. The PTFE membrane (effective area of $7.0 \times 10^{-3} \text{ m}^2$) was placed into an "LH-shaped" polyoxymethylene module working in a cross-flow mode in counter-current [16]. In a typical run, the CWPO-treated OMW (feed) and distilled water (permeate) were recirculated through heat and cool exchangers, respectively, by two peristaltic pumps working at a flow rate of 100 mL/min – Fig. 3. The initial operational conditions were selected based on the findings of a previous study [16]. Thermocouples placed at both sides of the DCMD module allowed to continuously monitor the cell temperature, which was maintained at $\approx 57 \text{ }^\circ\text{C}$ (feed side) and $\approx 18 \text{ }^\circ\text{C}$ (permeate side) throughout the experiments, resulting in a pressure differential of $\approx 16.5 \text{ kPa}$ between both sides [33]. Similar runs were also performed with feed temperatures of $\approx 66 \text{ }^\circ\text{C}$ and $\approx 75 \text{ }^\circ\text{C}$, resulting in $\Delta P \approx 26.2 \text{ kPa}$ and $\approx 41.0 \text{ kPa}$, respectively. The approximate values reported are due to small variations within the set temperature and cell temperature measured during the runs. The permeate fluxes across the membrane were determined by the change in weight of the permeate vial. The initial volumes of permeate (distilled water – DW) and retentate were 300 and 450 mL, respectively. In selected experiments, the retentate was also recirculated to the FBR unit (albeit in a discontinuous mode – dotted lines in Fig. 3) after the DCMD operation (typically 4 h runs) to treat the concentrated OMW produced in this step.

The total dissolved solids (TDS) were also measured over time on the permeate side with a conductivity meter (VWR mod. CO310), by multiplying the measured conductivity (mS) by a set TDS factor of 0.65. Experiments were conducted for 4 h and the permeate flux (J) was calculated for several time intervals following Eq. (1), where W is the mass of distillate – permeate (kg), A the effective membrane area (m^2), and t the sampling time (h).

The rejection (%) (R) was estimated following Eq. (2), where C_{permeate} is the concentration of any given lumped parameter (TOC, TPh, COD, or

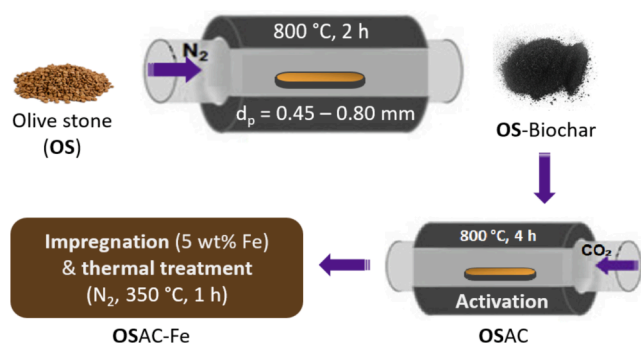


Fig. 1. Summarized scheme of the catalyst synthesis procedure adopted.

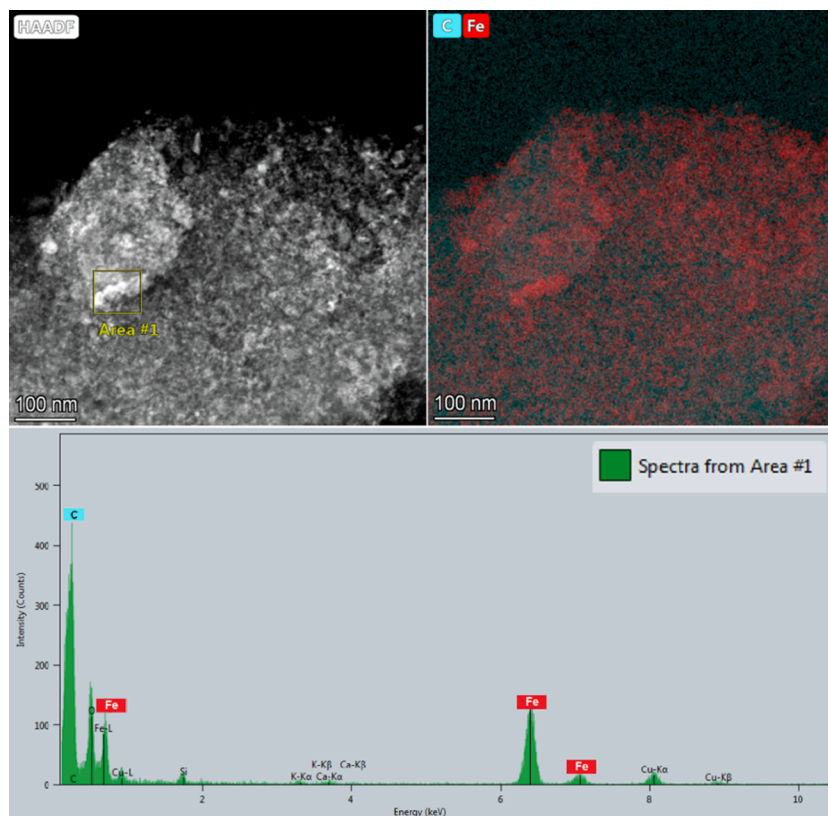


Fig. 2. Transmission electron microscopy micrograph with correspondent elemental mapping and EDX spectrum of the OSAC-Fe catalyst used.

Table 2

Main physicochemical characteristics of OMW supernatant before and after dilution (D). Legislated discharge limits for treated industrial wastewater and emission limits for water used for irrigation purposes shown for reference.

Parameter	OMW (supernatant)	OMW (D = 5-fold)	OMW (D = 7.5-fold)	Discharge limits*
pH	3.5 ± 0.3	4.0 ± 0.2	4.9 ± 0.1	6.9 – 9.0 ^(b)
COD (mg/L)	17 878 ± 554	3 562 ± 68	2 335 ± 54	150 ^(b)
BOD ₅ (mg/L)	3817 ± 483	970 ± 10	730 ± 10	25 ^(a) /40 ^(b)
TOC (mg/L)	6 685 ± 145	1258 ± 63	842 ± 45	n.e.
TPh (mg GA _{eq} /L)	1 098 ± 48	177 ± 17	143 ± 7	0.5 ^(b)
TSS (mg/L)	370 ± 40	130 ± 16	38 ± 6	35 ^(a) /60 ^(b)
TDS (mg/L)	2 120 ± 170	455 ± 17	338 ± 11	n.e.
Fe (mg/L)	1.05	0.23	0.16	2.0 ^(a, b)
Conductivity (µS/cm)	3 290 ± 120	703 ± 4	520 ± 7	n.e.
Turbidity (NTU)	408 ± 10	69 ± 5	51 ± 4	5 ^(a)
Color (1:20 dilution)	Visible	visible	visible	non-visible

*According to the Portuguese Decree-law 119/2019, 21st August – production of water for reuse in irrigation activities^(a), and Decree-law 236/98, 1st August in Annex XVIII – standards for industrial discharges^(b).
n.e. – not established.

TDS) of the permeate solution at a given time t , and $C_{feed,0}$ is the initial concentration of such parameter in the feed solution, respectively. The OMW concentration factor in the retentate side (β) was determined from Eq. (3).

$$J = \frac{\Delta W}{A \times \Delta t} \quad (1)$$

$$R(\%) = \left(1 - \frac{C_{permeate}(t)}{C_{feed_0}}\right) \times 100 \quad (2)$$

$$\beta = \frac{C_{retentate}(t)}{C_{feed_0}} \quad (3)$$

2.4. Analytical techniques

The physicochemical characterization of samples was performed following the Standard Methods of APHA [34], namely: Method 5220 D (closed reflux method) for COD determinations, using a heating block from Nanocolor (model Vario 4) and a photometer from Macherey-Nagel (model 500D); Method 5310 D for TOC analysis, using a Shimadzu TOC/TC apparatus (TOC-L model); Method 5210 B for BOD₅, using a WTW OxiTop Thermostat Box; TSS was determined by gravimetric analysis following Method 2540 B; quantification of dissolved iron was performed by flame atomic absorption spectrophotometry following Method 3111, using a model 939/959 AAS UNICAM spectrophotometer.

The total phenolic content (TPh) of the samples was estimated using the Folin–Ciocalteu reagent (Panreac) with gallic acid as the standard (values therein reported as mg GA_{eq}/L). In brief, 1 mL of sample was mixed with 5 mL of Folin–Ciocalteu reagent and 4 mL of Na₂CO₃ (7.5% w/v), and placed in the dark for 2 h; the color intensity was measured by spectrophotometry at 765 nm and the phenolic content determined from a calibration curve with known standards [35]. Hydrogen peroxide concentration was determined following the method developed by Sellers [36], using a Thermo Scientific spectrophotometer (model Genesys 10-S). Residual H₂O₂ in the samples causes an overestimation of the COD results, and thus a calibration curve was constructed to correct the results obtained according to Eq. (4):

$$COD_{corr} = COD - 0.468[H_2O_2]_{res} \quad (4)$$

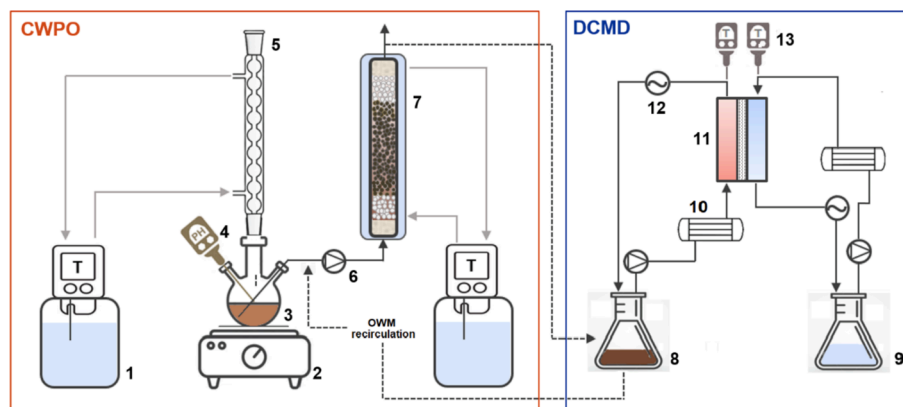


Fig. 3. Schematic representation of the combined experimental set-up: (1) recirculating water bath; (2) magnetic stirrer hot plate; (3) 3-neck flask with OMW + H_2O_2 ; (4) combined pH and temperature electrode; (5) reflux condenser; (6) peristaltic pump; (7) jacketed FBR; (8) retentate; (9) permeate; (10) heat/cool exchangers (both connected to separate recirculating water baths – not graphically represented); (11) DCMD module; (12) conductivity meter; (13) thermocouples.

Water contact angle determinations were performed with an optical tensiometer (Attension® model Theta) to evaluate the hydrophobicity of the membrane surface. The average contact angle was determined by the sessile drop method and three different regions in each membrane were evaluated to determine average values (tests performed with water, at room temperature, and using dried membrane samples).

3. Results and discussion

3.1. FBR experiments

One of the main limitations of membrane distillation operation is the rapid decrease of permeate flux due to the high concentration of solutes in the feed solution [37]. The variety and load of different organic compounds in the OMW feed matrix may also lead to membrane fouling (by deposition of dissolved or colloidal organic matter on the membrane surface) or scaling (by precipitation of sparingly soluble salts), which can cause wetting of the membrane and result in the free passage of contaminants through the pores [38,39]. A pre-treatment capable of reducing the effluent's initial load can prevent membrane fouling and

also scaling, as already suggested by V. Kumar *et al.* [40] for the management of secondary municipal wastewater.

In this study, the catalytic wet peroxide oxidation was considered as a pre-treatment step for continuous OMW depuration, and the effluent's COD, TPh, TOC, and residual H_2O_2 were monitored at the reactor outlet. Two set of experiments were performed with distinct OMW feed loadings, corresponding to a 5-fold dilution ($\text{COD}_0 = 3562 \pm 68 \text{ mg/L}$, $\text{TPh}_0 = 177 \pm 17 \text{ mg GA}_{\text{eq}}/\text{L}$) and a 7.5-fold dilution ($\text{COD}_0 = 2335 \pm 54 \text{ mg/L}$, $\text{TPh}_0 = 143 \pm 7 \text{ mg GA}_{\text{eq}}/\text{L}$) of the raw effluent supernatant (cf. Table 2). The fixed-bed reactor was fed continuously for 20 h, and the COD and TPh values registered at the outlet stream are shown in Fig. 4.

As mentioned before, different operational parameters – including oxidant dose (in the 0.75–3.0 g/L range), reaction temperature (varying from 20 to 60 °C), and volumetric flow rate (between 0.25 and 1.75 mL/min) – were previously optimized for a similar effluent and experimental set-up [14]; the main difference with the present study was the amount of catalyst loaded into the column (i.e., the contact time of the fluid with the catalyst was doubled). Therefore, the unreacted H_2O_2 in the outlet stream was reduced from 28% (as disclosed in the previous work to an

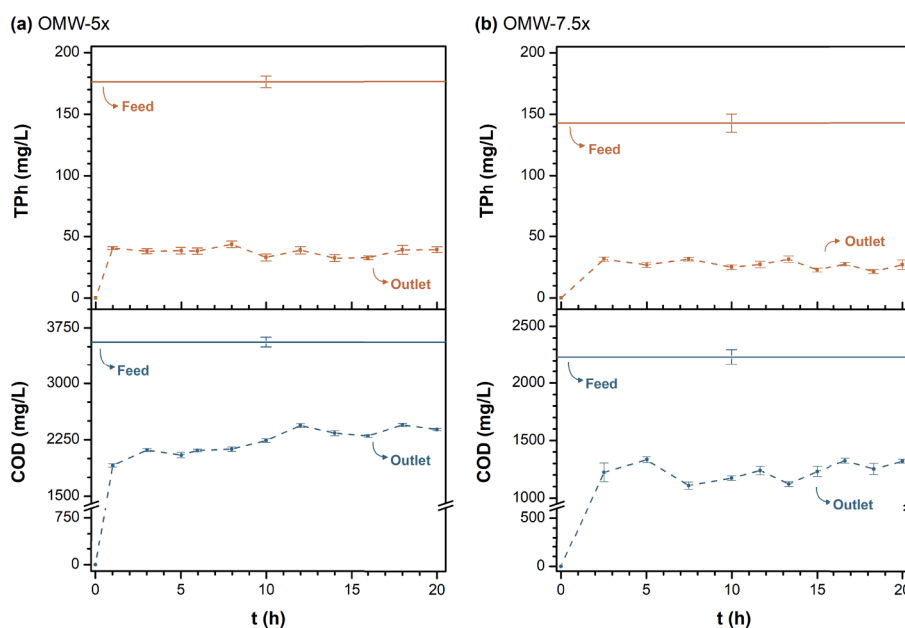


Fig. 4. COD and TPh concentrations over time at the FBR feed and outlet streams for (a) OMW-5 \times and (b) OMW-7.5 \times . Experimental conditions: $[\text{H}_2\text{O}_2]_{\text{feed}}/[\text{COD}]_{\text{feed}} = 2.3 \pm 0.1 \text{ g H}_2\text{O}_2/\text{g O}_2$, $W_{\text{cat}}/Q = 2.66 \text{ g min/mL}$, $T = 60 \text{ }^\circ\text{C}$, $Q = 0.75 \text{ mL/min}$, $\text{pH}_0 = 4.0 \pm 0.2$.

average of ca. 7% only of the initial dose in the run with OMW-5 \times (results not graphically presented for brevity). Similarly, higher oxidant conversions were observed throughout the entire run with OMW-7.5 \times , with steady-state FBR exit conversions >95%. Consequently, in both cases, the increase in catalyst amount also led to an overall improvement in the reduction of COD and TPh when compared to the efficiencies reported in the previous study (for instance, steady-state removals of 29% for COD and 60% for TPh were previously obtained with OMW-7.5 \times).

On average, removal efficiencies were slightly lower for the OMW with higher initial load (i.e., less diluted effluent – OMW-5 \times), with COD and TPh removals of 37% and 79%, respectively, whereas 45% and 81% reductions were obtained with OMW-7.5 \times at steady-state. As observed in Fig. 4, the TPh values reported at the reactor outlet were practically constant during the 20 h of operation, ranging from 32.4 to 41.7 mg GA_{eq}/L and 21.8–31.6 mg GA_{eq}/L, for OMW-5 \times and OMW-7.5 \times , respectively. The values of COD of the produced effluent were also maintained in the case of OMW-7.5 \times (ca. 1230 mg/L on average), whilst slightly increasing after \approx 10 h for OMW-5 \times (from an average of 2120 to 2360 mg/L). The higher variance in COD values at the reactor outlet is related to the presence of residual H₂O₂ that can cause an overestimation in the readings, tentatively eliminated through a calibration curve (Eq. (4)), though not possible for the entire range of H₂O₂ concentrations observed; this was particularly noticeable whenever higher concentrations of unreacted H₂O₂ were observed at the reactor outlet.

A smaller extent of TOC removal (mineralization) after CWPO was observed (removals of 14.2% and 16.8% for OMW-5 \times and OMW-7.5 \times , respectively), possibly related to the breakdown of suspended solids during the catalytic process, resulting in the dissolution of this fraction of organic matter to the solution (not previously accounted due to the sample's filtration before TOC analysis – i.e., dissolved organic carbon). This hypothesis was reinforced by the TDS values registered before (455 \pm 17 mg/L) and after oxidation (649 \pm 36 mg/L) in the case of the run performed with OMW-5 \times , along with a decrease in TSS (from 130 \pm 16 to 42 \pm 7 mg/L after CWPO). Furthermore, the values of BOD₅ also decrease by 86.6% to 130 \pm 10 mg/L. Similar trends were also observed for the CWPO-treated sample of OMW-7.5 \times (results not shown for brevity).

In both cases, the cumulative values of Fe dissolved in solution were found to be considerably higher than those observed in the original effluent (cf. Table 2), indicating some leaching of the metallic active phase from the catalyst. For instance, after 20 h of operation with OMW-5 \times , the iron dissolved in solution was 5.7 mg/L (corresponding to approximately 5 wt% of the initial Fe-load in the catalytic bed; similar weight percentage losses were obtained either with OMW-5 \times or OMW-7.5 \times). Although not significantly altering the process efficiency for the run time of the experiments reported here, Fe-leaching is typically known to cause catalytic activity loss in such heterogeneous Fenton-based processes [41]. The proposed integrated process may address this drawback to a certain extent, as the iron leached from the support can be maintained in the retentate side during the membrane operation, and may even be recirculated to the FBR unit afterward, promoting the homogeneous Fenton process. Still, other factors must be taken into account to evaluate the catalyst deactivation, including the poisoning of active sites by adsorption of intermediate/final oxidation products and/or heteroatoms (also previously witnessed for the treatment of a polyphenolic synthetic solution, where the enrichment of C–O bonds characteristic of phenolic compounds was observed by XPS analysis of a spent catalyst sample [14]), and/or the formation of deposits that reduce the specific surface area of the material (limiting the accessibility of oxidant/contaminant molecules to active Fe-sites within the catalyst's porous structure) [42].

Despite the removals achieved by oxidation, the produced effluents are still non-compliant with legislated emission values for wastewater discharge into natural bodies of water (Portuguese Decree-law 236/98).

Nonetheless, the main goal of this step was to produce a continuous stream of pre-treated OMW with steady physicochemical properties over time (e.g., COD and TPh), and then check its suitability for further depuration through membrane distillation with simultaneous water recovery.

3.2. DCMD experiments

The performance of DCMD for the management of different OMW streams was evaluated by the transmembrane fluxes achieved, the rejection values, and the overall quality of the permeate streams produced. A run with DW was also performed to assess the maximum permeate flux (J) of the distillation module in the absence of membrane fouling, under a defined set of operational conditions ($Q_{\text{feed}} = Q_{\text{permeate}} = 100$ mL/min, $T_{\text{feed}} \approx 57$ °C, $T_{\text{permeate}} \approx 18$ °C, $t = 4$ h). Permeate fluxes and water recovery calculated along time for the two untreated OMW samples (OMW-5 \times and OMW-7.5 \times), as well as for the corresponding CWPO-treated samples of OMW, are shown in Fig. 5.

After stabilization of the temperature gradient inside the membrane module (i.e., after ca. 20 min) the flux of DW was maintained practically unaltered at \approx 10.5 kg/m² h for the experimental conditions tested (Fig. 5a). Contrarily, different degrees of flux decline were observed for both untreated and CWPO-treated samples of OMW. Due to the initial composition of OMW comprising several organic (and inorganic) solutes, a lower water vapor pressure is foreseen and thus also smaller permeation fluxes values in comparison to that of DW [23]. Expectably, OMW-5 \times (the less diluted effluent) registered the highest permeation flux decline after 4 h of operation (ca. 60%), whereas this value was close to 48% for the more diluted untreated sample (OMW-7.5 \times).

After 4 h of operation, the system achieved similar H₂O recoveries for samples with lower initial loadings (which included the CWPO-treated OMW-5 \times with similar COD and TOC values as the untreated OMW-7.5 \times) – Fig. 5b. Still, the recoveries were always lower than the one achieved with DW (final recovery of ca. 58%). A very distinct profile was obtained in the OMW-5 \times , which also presented the lowest productivity (ca. 38%).

The higher flux decline (and lower H₂O recovery) observed for the sample with higher organic load (OMW-5 \times) could be partially attributed to the phenomena of concentration polarization occurring due to the rapid increase in solute concentration over time in the retentate side that leads to a decrease in the driving force (i.e., partial vapor pressure) [15]. Additionally, the deposition of particulate matter on the membrane surface (membrane scaling and/or organic fouling) – visually confirmed after the experiments, cf. Fig. 6 – suggests the occurrence of a more extensive pore-blocking in this sample.

Increased resistance of water vapor transport across the membrane over time is therefore expected, and under such conditions membrane wetting is also possible, further hindering the process efficiency. Wetting phenomena occurs when the transmembrane pressure (ΔP) exceeds the liquid entry pressure (LEP), allowing for the feed to pass through the membrane pores. Among others, LEP is directly influenced by the membrane contact angle and water surface tension, and thus a decrease in both parameters can facilitate membrane wetting. Since the degradation of organic contaminants causes an increase in surface tension that may impede their interaction with the hydrophobic membrane surface [38], the oxidative pre-treatment could be potentially responsible for this phenomenon, thus allowing for higher fluxes.

The measurement of membrane contact angles provided evidence of this phenomenon. For example, in the case of OMW-7.5 \times , the used membrane presented an average contact angle of 106.0° (measured at the center of the membrane) while this value was clearly improved by the oxidative pre-treatment step to 142.4° (also measured at the center of the membrane). Comparatively, a pristine PTFE membrane exhibits a contact angle of 145.8°, confirming its highly hydrophobic character. The observed behavior is in line with similar reports in the literature for this type of effluent [22,37].

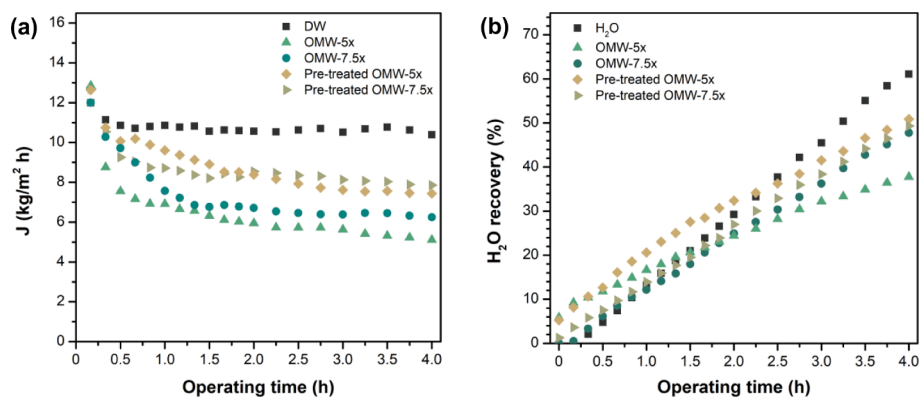


Fig. 5. (a) DCMD permeate flux and (b) H₂O recovery over time for DW and for OMW samples (non-treated and pre-treated by CWPO). Experimental conditions: $T_{\text{feed}} \approx 57$ °C and $T_{\text{permeate}} \approx 18$ °C ($\Delta P \approx 16.5$ kPa), $Q = 100$ mL/min.

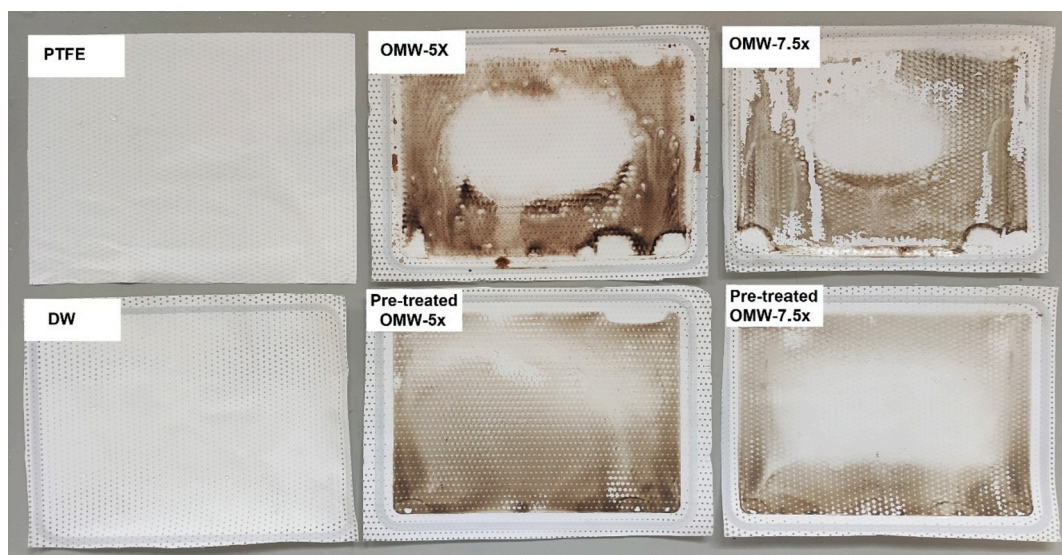


Fig. 6. Visual comparison of a neat-PTFE membrane with the used ones in DCMD after 4 h of operation for the different feed solutions tested. Experimental conditions: $T_{\text{feed}} \approx 57$ °C and $T_{\text{permeate}} \approx 18$ °C ($\Delta P \approx 16.5$ kPa), $Q = 100$ mL/min.

The extent of membrane scaling and/or fouling is visibly dependent on the initial load of the effluent, but more importantly, on the oxidative pre-treatment step, as highlighted in Fig. 6. The resulting brownish coloration that appears on the membrane surface – noticeably darker in the case of untreated OMW samples – is probably related to the presence of lignin polymerized with phenolic compounds, and constitutes the most resistant fraction of OMW [7,43]. The contact angles observed in such spots are considerably lower than those previously reported for the center of the membrane, with measured average contact angles as low as 45.4° in areas where fouling/scaling is more severe (predominantly in the membrane edges, due to the module's intrinsic design and operation). In general, a less concentrated fouling layer was obtained in the membrane surface of pre-treated samples, expectably as a result of the phenolic content reductions achieved by the CWPO step.

Despite the resemblances in the permeate fluxes obtained for both pre-treated samples, with $J \approx 7.4$ kg/m² h after 4 h, the catalytic pre-treatment step resulted in a clear improvement of the fluxes obtained in comparison to those of the respective untreated samples. El-Abbassi *et al.* [23] reported a similar behavior for pre-treated samples of OMW via microfiltration and coagulation/flocculation, whereas the work of Farinelli *et al.* [38] showed no specific advantage in the obtained water fluxes by using the homogenous Fenton oxidation as a preliminary stage for the DCMD of hypersaline “produced water” from oil and gas extraction activities.

Both permeate (Table 3) and retentate (Table 4) streams were analyzed to evaluate the efficiency of the DCMD process in the production of water and concentration of contaminants, respectively. In addition to the improvement in productivity of the DCMD unit by the pre-oxidation step of the raw OMW (higher H₂O recovery *cf.* Fig. 5b), the resulting water quality after the combined process was also enhanced when compared to that of the membrane distillation stage alone. Table 3 shows the characterization of the produced streams of permeate obtained by untreated samples of OMW-5x and OMW-7.5x, as well as the respective CWPO-treated ones. Rejection percentages achieved by the membrane distillation step alone and the combined process (oxidation and membrane distillation) are highlighted between brackets. It is worth noting that the dilution effect occurring in the permeate vial due to the initial volume of DW (300 mL) was taken into consideration and eliminated for the calculation of the concentrations and rejection percentages presented.

The characterization results of both OMW samples show that the DCMD unit *per se* was able to effectively reduce COD, TPh, and TOC in the permeate stream to a similar degree, independently of whether the effluent was pre-treated or not. However, the absolute values of all parameters evaluated were significantly improved by the combined process (and thus also the respective removal efficiencies by comparison to the DCMD step alone, as highlighted in the columns labelled as “CWPO + DCMD” of Table 3). Comparing the global rejection efficiencies (i.e.,

Table 3

Permeate characterization after 4 h of DCMD; rejection % shown between brackets. Experimental conditions: $T_{\text{feed}} \approx 57^\circ\text{C}$ and $T_{\text{permeate}} \approx 18^\circ\text{C}$ ($\Delta P \approx 16.5$ kPa), $Q = 100$ mL/min.

Parameter	OMW-5×	OMW-7.5×	Pre-treated OMW-5×		Pre-treated OMW-7.5×	
	DCMD step		DCMD step	CWPO + DCMD	DCMD step	CWPO + DCMD
COD (mg/L)	466 (87.1%)	290 (88.4%)	329 (86.2%)	(90.8%)	265 (85.0%)	(89.2%)
TPh (mg GA _{eq} /L)	1.7 (99.1%)	0 (100%)	0.5 (98.9%)	(99.7%)	0 (100%)	(100%)
TOC (mg/L)	249 (78.7%)	199 (76.4%)	220 (78.6%)	(81.6%)	188 (73.1%)	(77.8%)
TDS (mg/L)	41.0 (91.0%)	38.8 (90.0%)	68.4 (88.8%)	(85.0%)	52.6 (91.4%)	(84.4%)

Table 4

Retentate characterization after 4 h of DCMD; concentration factors of the retentate ($\beta_{4\text{ h}}$) shown in brackets. Experimental conditions: $T_{\text{feed}} \approx 57^\circ\text{C}$ and $T_{\text{permeate}} \approx 18^\circ\text{C}$ ($\Delta P \approx 16.5$ kPa), $Q = 100$ mL/min.

Parameter	OMW-5×	OMW-7.5×	Pre-treated OMW-5×	Pre-treated OMW-7.5×
	COD (mg/L)	7111 (2.0)	4501 (1.8)	4337 (1.8)
TPh (mg GA _{eq} /L)	517.9 (2.9)	375.1 (2.6)	154.5 (3.3)	80.3 (3.2)
TOC (mg/L)	2729 (2.3)	1776 (2.1)	2092 (2.0)	1198 (1.7)
TDS (mg/L)	1085 (2.4)	785 (1.7)	839 (1.4)	988 (1.6)

after CWPO + DCMD) achieved with OMW-5× and OMW-7.5×, the rejection percentages obtained were similar independently of the effluent's organic load after oxidation. The TDS concentrations registered were also small in comparison to the feed solutions, albeit a higher percentage of TDS rejection was attained for the non-treated samples. This behavior was probably due to the breakdown of suspended solids that occurred after CWPO, as mentioned in Section 3.1. In both cases, to a greater or lesser extent, the characterization of the permeate side suggests the presence of volatile compounds in the wastewater matrixes (accounted for as COD and TOC) that could also have resulted from the free passage through the membrane pores, or the occurrence of membrane wetting previously discussed. Though not referred to in Table 3, the concentration of Fe dissolved in the permeate was also very low in all cases (<0.08 mg/L), thus also providing a key advantage to the integrated process, as the Fe resulting from the catalyst leaching in the catalytic step is almost exclusively maintained in the retentate side. Moreover, no residual H₂O₂ was detected in the permeate stream analysis after the integrated process, which could be potentially linked to its thermal degradation during the DCMD operation.

Values of the concentration factors after 4 h of operation ($\beta_{4\text{ h}}$, Table 4) point out the more denoted effect of the concentration polarization effect referred earlier, as slightly higher concentration factors of COD, TOC and TDS were obtained for the untreated samples of OMW. The retentate concentration factors obtained were in line with the water recovery in the permeate side previously shown (Fig. 5b). Oppositely, a significantly higher TPh concentration factor in DCMD was observed after processing both untreated and pre-treated samples, potentially explained by the "aggregation" of the phenolic fraction of the wastewater to the TSS one, and that ended up dissolved in solution by the process temperature (in line with the TDS values observed). A similar range of concentration factors was reported by other authors [23,24] for specific OMW phenolic compounds (namely, gallic acid and tyrosol), while others (such as oleuropein) presented considerably smaller β values.

To take advantage of the effluent's temperature after the CWPO step, the membrane unit was initially operated at $T_{\text{feed}} \approx 57^\circ\text{C}$. Still, DCMD is

a thermally driven process and an increase in ΔT is expected to favor the process efficiency, as per previous reports [23,37,39]. In an attempt to further improve the permeate flux and quality of the permeate stream to meet legislated emission values for irrigation purposes (Table 2), further experiments were conducted with pre-treated samples of OMW-7.5×. Fixing T_{permeate} at $\approx 18^\circ\text{C}$, two additional feed temperatures were tested ($T_{\text{feed}} \approx 66$ and $\approx 75^\circ\text{C}$) resulting in pressure differentials of ≈ 26.2 and ≈ 41.0 kPa, respectively. Permeate fluxes and TDS rejection values over time are shown in Fig. 7.

Increasing the feed temperature by ca. 10 °C resulted in 60% improvement of the permeate flux, which was more than doubled when the mean bulk temperature was increased by ca. 20 °C – Fig. 7a. The TDS rejections (R) – Fig. 7b – were always below the theoretical maximum and slowly decreased over time in every case to a similar extent, which can be partially attributed to the wetting of the membrane pores [17,44]. It is also worth noting that due to the higher permeate fluxes achieved at higher feed temperatures, the system operation was limited to the fixed initial volume of solution fed to the DCMD unit (450 mL), and thus the values reported in Fig. 8 were equitably compared for an operating time of 3 h.

As to the quality of permeate streams obtained after the integrated process reported in Fig. 8, all parameters evaluated varied in a close range of values independently of the feed temperature used (and thus transmembrane pressure). This behavior, in addition to the higher permeate fluxes achieved as ΔP increases (Fig. 7a), can be advantageously adopted to produce higher volume of permeate over time with steady physicochemical properties, although the higher energy costs associated with heating the feed solution may need to be taken into consideration.

The permeate water obtained under the conditions tested was able to meet several criteria thresholds required for direct discharge into water bodies according to Portuguese legislation (cf. Table 2), including TPh (<0.11 mg GA_{eq}/L), TSS (<10 mg/L) and Fe (<0.08 mg/L) concentrations in all cases. The BOD₅ values reported in the permeate streams also met the criteria when operating at $\Delta P \approx 26.2$ kPa (<40 mg/L), or were found to be slightly above the emission values in the remaining cases (74 – 87 mg/L). Likewise, the values of COD obtained were still above the limit emission value of 150 mg/L (e.g., 265 ± 9 mg/L in the best scenario, i.e. $\Delta P \approx 16.5$ kPa – Fig. 8). As to the legal scheme for the "production of water for its reuse, obtained from the treatment of wastewater, in the irrigation of crops" from the Portuguese Decree-law 119/2019, values of turbidity (<4.1 NTU), TSS and Fe were also always below the imposed discharge limits, but the more restrictive value for BOD₅ (i.e., below 25 mg/L) was not achieved under the conditions tested.

3.3. DCMD-retentate recirculation to the FBR

Notwithstanding the achieved quality parameters of the permeate water produced, the DCMD operation also generates a secondary stream of concentrated waste (i.e., the retentate) that requires downstream handling; in fact, the management of such process' by-product is often

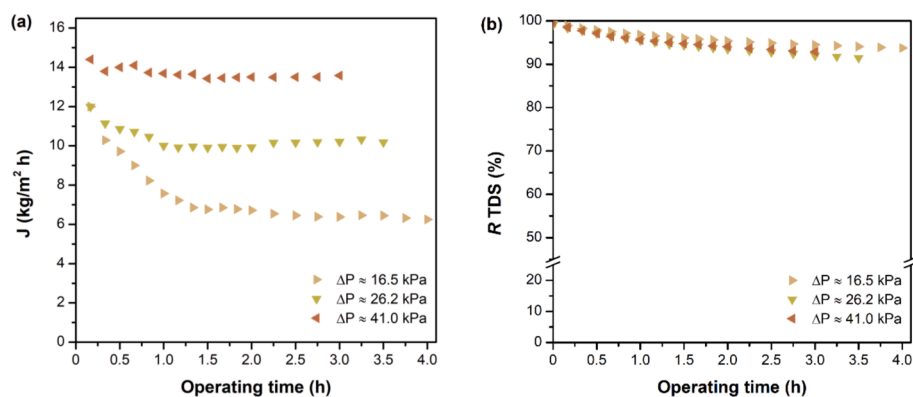


Fig. 7. (a) DCMD permeate flux and (b) TDS rejection over time for CWPO pre-treated samples of OMW-7.5 \times . Experimental conditions: $T_{\text{permeate}} \approx 18^\circ\text{C}$, $Q = 100$ mL/min.

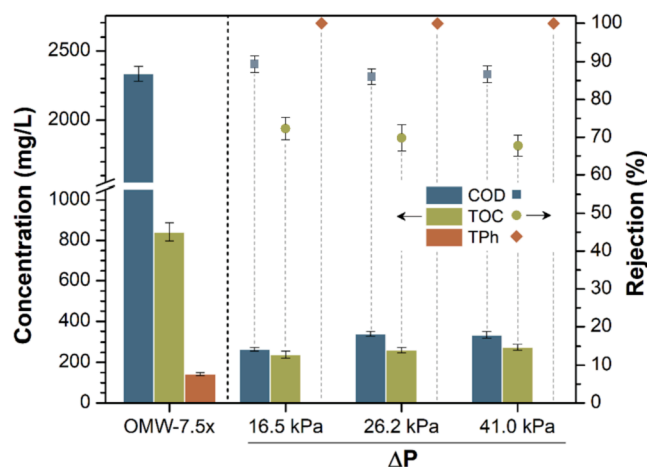


Fig. 8. Concentration of COD, TOC, and TPh (permeate) after the integrated process (CWPO + DCMD), initial values of OMW-7.5 \times presented for reference. Right y-axis shows the global rejection for each parameter. Experimental conditions: $T_{\text{permeate}} \approx 18^\circ\text{C}$, $Q = 100$ mL/min, $t = 3$ h (error bars: standard errors of the means, $n = 3$).

disregarded in similar reports. On another hand, it was previously shown by the authors [14] that for a similar experimental set-up (only differing in the amount of catalyst loaded into the FBR), the CWPO process was able to maintain similar treatment efficiencies independently of OMW initial load (for COD_0 values ranging from 594 to 3595 mg/L).

Therefore, three distinct DCMD-retentate solutions were re-circulated (albeit in discontinuous mode) from the membrane unit back to the catalytic reactor (i.e., the DCMD run was stopped after 4 h, and the resulting retentate was collected and used to feed the FBR). Fig. 9 highlights the main properties (COD, TOC, and TPh) of the retentate samples after the catalytic step (i.e., FBR outlet at steady-state). The results obtained are in good agreement with the previous findings. The overall similar range of COD (37.4–42.7%), TOC (32.2–33.2%), and TPh (77.4–83.9%) removals after the recirculation to the FBR, independently of the initial OMW-DCMD retentate load (COD_0 range of 2689–7111 mg/L), confirms the good adjustment between the $[\text{H}_2\text{O}_2]/[\text{COD}]$ feed ratio and contact time selected for the FBR operation. Moreover, identical COD and TPh removal percentages were obtained with either samples that were treated by FBR-DCMD-FBR, or retentate samples after DCMD-FBR alone (i.e., OMW-5 \times retentate *cf.* displayed in Fig. 9, or OMW-7.5 \times , as reported in Section 3.1). Finally, an improvement in TOC removal efficiencies by *ca.* 2-fold after the membrane distillation process was also achieved (previously in the 14.2–16.8% range *cf.*

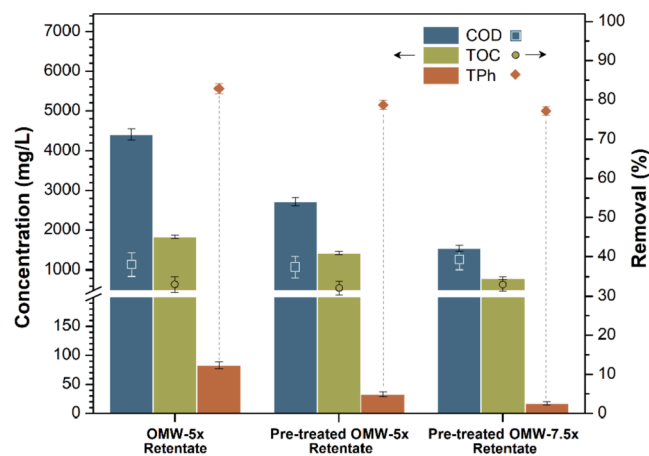


Fig. 9. COD, TOC, and TPh of different retentates after recirculation to the FBR with indication of oxidation efficiencies in steady-state (yy-axis). DCMD experimental conditions: $T_{\text{feed}} \approx 57^\circ\text{C}$, $T_{\text{permeate}} \approx 18^\circ\text{C}$, $\Delta P \approx 16.5$ kPa, $Q = 100$ mL/min; FBR: $[\text{H}_2\text{O}_2]_{\text{feed}}/[\text{COD}]_{\text{feed}} = 2.3 \pm 0.1$ g $\text{H}_2\text{O}_2/\text{g O}_2$, $W_{\text{cat}}/Q = 2.66$ g min/mL, $T = 60^\circ\text{C}$, $Q = 0.75$ mL/min, $\text{pH}_0 = 4.0 \pm 0.2$ (error bars: standard errors of the means, $n = 3$).

results in Section 3.1 for FBR alone, to 32.2–33.2% as depicted in Fig. 9 for FBR-DCMD-FBR). This enhancement can be justified by the fact that the most hardly degradable compounds were adhered to the membrane (*cf.* Fig. 6) and also by the transference of some organic solutes to the permeate side (Table 3).

4. Conclusions

This work highlighted the potential of a combined treatment process for OMW management comprising a preliminary oxidative step by CWPO in a fixed-bed reactor and the subsequent recovery of water by DCMD. The pre-treated samples of OMW allowed the operation of the membrane distillation unit at higher fluxes than those registered for analogous untreated samples, due to the oxidation of organic matter and breakdown of suspended matter. The integrated process also showed globally higher rejections of organic matter from the feed solutions when compared to the operation of each process alone. A more accentuated flux decline in the initial stages of the process (i.e., after 1 h) was observed when using non-treated samples of OMW, as a consequence of the higher initial organic load. Further improvement to the permeate flux of pre-treated samples was possible by increasing the feed temperature (at a fixed permeate temperature), but no clear correlation could be established for the resulting permeate quality. In any case, the produced permeate water stream showed several parameters that

comply with legislated values for discharge into water bodies, including TSS, Tph, BOD₅, and dissolved Fe, while COD values were always slightly higher than the threshold defined by legislation despite the high removal efficiencies obtained (>89%). The produced DCMD-retentates (with ca. double the organic load of the original OMW samples) were also successfully treated by the same CWPO process employed earlier (i.e., FBR-DCMD-FBR), with maximum removal percentages of 42.7% for COD, 83.9% for Tph, and 33.2% for TOC (i.e., similar to those obtained previously with the original OMW samples). Therefore, this work reports on the management of all residues generated, in a waste-to-value perspective.

Declaration of Competing Interest

The authors declare that they have no known competing financial interests or personal relationships that could have appeared to influence the work reported in this paper.

Data availability

The authors are unable or have chosen not to specify which data has been used.

Acknowledgments

This work was financially supported by: LA/P/0045/2020 (ALICE), UIDB/00511/2020 and UIDP/00511/2020 (LEPABE), funded by national funds through FCT/MCTES (PIDDAC); project VERPRAZ (NORTE-01-0247-FEDER-39789) funded by European Regional Development Funds (ERDF) through North Portugal Regional Operational Programme (NORTE 2020); project Healthy Waters (NORTE-01-0145-FEDER-000069) supported by NORTE 2020 under the PORTUGAL 2020 Partnership Agreement through ERDF, and the project ref. RTI2018-099224-B-I00 from MCIN/AEI/10.13039/501100011033/FEDER “Una manera de hacer Europa”. This work was also financially supported by: Base-UIDB/50020/2020 and Programmatic-UIDP/50020/2020 Funding of LSRE-LCM, funded by national funds through FCT/MCTES (PIDDAC). Bruno Esteves is grateful to FCT for financial support through the PhD grant (SFRH/BD/129235/2017), with financing from National and the European Social Funds through the Human Capital Operational Programme (POCH). Sergio Morales-Torres acknowledges the MCIN/AEI/10.13039/501100011033, and the European Social Found (FSE) “El FSE invierte en tu futuro” for a Ramón y Cajal research contract (RYC-2019-026634I).

References

- [1] S. Casani, M. Rouhany, S. Knöchel, A discussion paper on challenges and limitations to water reuse and hygiene in the food industry, *Water Res.* 39 (2005) 1134–1146, <https://doi.org/10.1016/j.watres.2004.12.015>.
- [2] E. Chatzisyneon, S. Foteinis, D. Mantzavinos, T. Tsoutsos, Life cycle assessment of advanced oxidation processes for olive mill wastewater treatment, *J. Clean. Prod.* 54 (2013) 229–234, <https://doi.org/10.1016/j.jclepro.2013.05.013>.
- [3] M.M. Mekonnen, A.Y. Hoekstra, The green, blue and grey water footprint of crops and derived crop products, *Hydrol. Earth Syst. Sci.* 15 (2011) 1577–1600, <https://doi.org/10.5194/hess-15-1577-2011>.
- [4] FAOSTAT - Food and Agriculture Organization Corporate Statistical Database, (2022). <http://www.fao.org/statistics/en/> (accessed January 2, 2022).
- [5] A.G. Vlyssides, M. Loizides, P.K. Karlis, Integrated strategic approach for reusing olive oil extraction by-products, *J. Clean. Prod.* 12 (2004) 603–611, [https://doi.org/10.1016/S0959-6526\(03\)00078-7](https://doi.org/10.1016/S0959-6526(03)00078-7).
- [6] A.Y. Gebreyohannes, R. Mazzei, L. Giorno, Trends and current practices of olive mill wastewater treatment: Application of integrated membrane process and its future perspective, *Sep. Purif. Technol.* 162 (2016) 45–60, <https://doi.org/10.1016/j.seppur.2016.02.001>.
- [7] S. Dermeche, M. Nadour, C. Larroche, F. Moulti-Mati, P. Michaud, Olive mill wastes: Biochemical characterizations and valorization strategies, *Process Biochem.* 48 (2013) 1532–1552, <https://doi.org/10.1016/j.procbio.2013.07.010>.
- [8] T.M. Koutsos, T. Chatzistathis, E.I. Balampekou, A new framework proposal, towards a common EU agricultural policy, with the best sustainable practices for the re-use of olive mill wastewater, *Sci. Total Environ.* 622–623 (2018) 942–953, <https://doi.org/10.1016/j.scitotenv.2017.12.073>.
- [9] R.A. Fragoso, E.A. Duarte, Reuse of drinking water treatment sludge for olive oil mill wastewater treatment, *Water Sci. Technol.* 66 (2012) 887–894, <https://doi.org/10.2166/wst.2012.267>.
- [10] E. Neyens, J. Baeyens, A review of classic Fenton’s peroxidation as an advanced oxidation technique, *J. Hazard. Mater.* 98 (2003) 33–50, [https://doi.org/10.1016/S0304-3894\(02\)00282-0](https://doi.org/10.1016/S0304-3894(02)00282-0).
- [11] S. Navalon, M. Alvaro, H. Garcia, Heterogeneous Fenton catalysts based on clays, silicas and zeolites, *Appl. Catal. B Environ.* 99 (2010) 1–26, <https://doi.org/10.1016/j.apcatb.2010.07.006>.
- [12] S. Rahim Pouran, A.A. Abdul Raman, W.M.A. Wan Daud, Review on the application of modified iron oxides as heterogeneous catalysts in Fenton reactions, *J. Clean. Prod.* 64 (2014) 24–35, <https://doi.org/10.1016/j.jclepro.2013.09.013>.
- [13] B.M. Esteves, S. Morales-Torres, F.J. Maldonado-Hódar, L.M. Madeira, Integration of olive stones in the production of Fe/AC-catalysts for the CWPO treatment of synthetic and real olive mill wastewater, *Chem. Eng. J.* 411 (2021), 128451, <https://doi.org/10.1016/j.cej.2021.128451>.
- [14] B.M. Esteves, S. Morales-Torres, F.J. Maldonado-Hódar, L.M. Madeira, Sustainable iron-olive stone-based catalysts for Fenton-like olive mill wastewater treatment: development and performance assessment in continuous fixed-bed reactor operation, *Chem. Eng. J.* 435 (2022), 134809, <https://doi.org/10.1016/j.cej.2022.134809>.
- [15] M. Khayet, Membranes and theoretical modeling of membrane distillation: A review, *Adv. Colloid Interface Sci.* 164 (2011) 56–88, <https://doi.org/10.1016/j.cis.2010.09.005>.
- [16] T.L.S. Silva, S. Morales-Torres, C.M.P. Esteves, A.R. Ribeiro, O.C. Nunes, J. L. Figueiredo, A.M.T. Silva, Desalination and removal of organic micropollutants and microorganisms by membrane distillation, *Desalination.* 437 (2018) 121–132, <https://doi.org/10.1016/j.desal.2018.02.027>.
- [17] M.S. El-Bourawi, Z. Ding, R. Ma, M. Khayet, A framework for better understanding membrane distillation separation process, *J. Memb. Sci.* 285 (2006) 4–29, <https://doi.org/10.1016/j.memsci.2006.08.002>.
- [18] B.L. Pangarkar, M.G. Sane, M. Guddad, Reverse osmosis and membrane distillation for desalination of groundwater: a review, *ISRN Mater. Sci.* 2011 (2011) 1–9, <https://doi.org/10.5402/2011/523124>.
- [19] O. Aime Mudimu, M. Peters, F. Brauner, G. Braun, Overview of membrane processes for the recovery of polyphenols from olive mill wastewater, *Am. J. Environ. Sci.* 8 (2012) 195–201.
- [20] M.C. Carnevale, E. Gnisci, J. Hilal, A. Criscuoli, Direct Contact and Vacuum Membrane Distillation application for the olive mill wastewater treatment, *Sep. Purif. Technol.* 169 (2016) 121–127, <https://doi.org/10.1016/j.seppur.2016.06.002>.
- [21] A. El-Abbassi, A. Hafidi, M.C. García-Payo, M. Khayet, Concentration of olive mill wastewater by membrane distillation for polyphenols recovery, *Desalination.* 245 (2009) 670–674, <https://doi.org/10.1016/j.desal.2009.02.035>.
- [22] A. El-Abbassi, H. Kiai, A. Hafidi, M.C. García-Payo, M. Khayet, Treatment of olive mill wastewater by membrane distillation using polytetrafluoroethylene membranes, *Sep. Purif. Technol.* 98 (2012) 55–61, <https://doi.org/10.1016/j.seppur.2012.06.026>.
- [23] A. El-Abbassi, A. Hafidi, M. Khayet, M.C. García-Payo, Integrated direct contact membrane distillation for olive mill wastewater treatment, *Desalination.* 323 (2013) 31–38, <https://doi.org/10.1016/j.desal.2012.06.014>.
- [24] E. Garcia-Castello, A. Cassano, A. Criscuoli, C. Conidi, E. Drioli, Recovery and concentration of polyphenols from olive mill wastewaters by integrated membrane system, *Water Res.* 44 (2010) 3883–3892, <https://doi.org/10.1016/j.watres.2010.05.005>.
- [25] R. Tundis, C. Conidi, M.R. Loizzo, V. Sicari, R. Romeo, A. Cassano, Concentration of bioactive phenolic compounds in olive mill wastewater by direct contact membrane distillation, *Molecules.* 26 (2021) 1808, <https://doi.org/10.3390/molecules26061808>.
- [26] Regulation (EU) 2020/741 of the European Parliament and of the Council of 25 May 2020 on minimum requirements for water reuse, 2020.
- [27] X. Liu, X.T. Bi, C. Liu, Y. Liu, Performance of Fe/AC catalyst prepared from demineralized pine bark particles in a microwave reactor, *Chem. Eng. J.* 193–194 (2012) 187–195, <https://doi.org/10.1016/j.cej.2012.04.039>.
- [28] R.C. Martins, T. Gomes, R.M. Quinta-ferreira, Fenton’s depuration of weathered olive mill wastewaters over a Fe-Ce-O solid catalyst, *Ind. Eng. Chem. Res.* 49 (2010) 9043–9051, <https://doi.org/10.1021/ie101203p>.
- [29] M.S. Lucas, J.A. Peres, Removal of COD from olive mill wastewater by Fenton’s reagent: Kinetic study, *J. Hazard. Mater.* 168 (2009) 1253–1259, <https://doi.org/10.1016/j.jhazmat.2009.03.002>.
- [30] S. Morales-Torres, T.L.S. Silva, L.M. Pastrana-Martínez, A.T.S.C. Brandão, J. L. Figueiredo, A.M.T. Silva, Modification of the surface chemistry of single- and multi-walled carbon nanotubes by HNO₃ and H₂SO₄ hydrothermal oxidation for application in direct contact membrane distillation, *Phys. Chem. Chem. Phys.* 16 (2014) 12237–12250, <https://doi.org/10.1039/c4cp00615a>.
- [31] S. Zare, A. Kargari, Membrane properties in membrane distillation, Elsevier Inc., 2018. doi:10.1016/B978-0-12-815818-0.00004-7.
- [32] L. Eykens, K. De Sitter, C. Dotremont, L. Pinoy, B. Van Der Bruggen, How to optimize the membrane properties for membrane distillation: a review, *Ind. Eng. Chem. Res.* 55 (2016) 9333–9343, <https://doi.org/10.1021/acs.iecr.6b02226>.
- [33] J. Zhang, N. Dow, M. Duke, E. Ostarcevic, J. De Li, S. Gray, Identification of material and physical features of membrane distillation membranes for high performance desalination, *J. Memb. Sci.* 349 (2010) 295–303, <https://doi.org/10.1016/j.memsci.2009.11.056>.
- [34] APHA, AWWA, WEF, Standard methods for the examination of water and wastewater, 22nd ed., American Public Health Association, Washington, DC, 2012.

- [35] B.M. Esteves, C.S.D. Rodrigues, L.M. Madeira, Synthetic olive mill wastewater treatment by Fenton's process in batch and continuous reactors operation, *Environ. Sci. Pollut. Res.* 25 (2018) 34826–34838, <https://doi.org/10.1007/s11356-017-0532-y>.
- [36] R.M. Sellers, Spectrophotometric determination of hydrogen peroxide using potassium titanium(IV) oxalate, *Analyst.* 105 (1980) 950–954, <https://doi.org/10.1039/an9800500950>.
- [37] H. Kiai, M.C. García-Payo, A. Hafidi, M. Khayet, Application of membrane distillation technology in the treatment of table olive wastewaters for phenolic compounds concentration and high quality water production, *Chem. Eng. Process. Process Intensif.* 86 (2014) 153–161, <https://doi.org/10.1016/j.cep.2014.09.007>.
- [38] G. Farinelli, M. Coha, M. Minella, D. Fabbri, M. Pazzi, D. Vione, A. Tiraferri, Evaluation of Fenton and modified Fenton oxidation coupled with membrane distillation for produced water treatment: Benefits, challenges, and effluent toxicity, *Sci. Total Environ.* 796 (2021), 148953, <https://doi.org/10.1016/j.scitotenv.2021.148953>.
- [39] L.D. Nghiem, T. Cath, A scaling mitigation approach during direct contact membrane distillation, *Sep. Purif. Technol.* 80 (2011) 315–322, <https://doi.org/10.1016/j.seppur.2011.05.013>.
- [40] R. Vinoth Kumar, M.O. Barbosa, A.R. Ribeiro, S. Morales-Torres, M.F.R. Pereira, A. M.T. Silva, Advanced oxidation technologies combined with direct contact membrane distillation for treatment of secondary municipal wastewater, *Process Saf. Environ. Prot.* 140 (2020) 111–123, <https://doi.org/10.1016/j.psep.2020.03.008>.
- [41] Y. Zhu, R. Zhu, Y. Xi, J. Zhu, G. Zhu, H. He, Strategies for Enhancing the Heterogeneous Fenton Catalytic Reactivity: A review, *Appl. Catal. B Environ.* 255 (2019), 117739, <https://doi.org/10.1016/j.apcatb.2019.05.041>.
- [42] M. Lu, Y. Yao, L. Gao, D. Mo, F. Lin, S. Lu, Continuous treatment of phenol over an Fe₂O₃/γ-Al₂O₃ catalyst in a fixed-bed reactor, *Water, Air, Soil Pollut.* 226 (2015), <https://doi.org/10.1007/s11270-015-2363-0>.
- [43] H. Zbakh, A. El Abbassi, Potential use of olive mill wastewater in the preparation of functional beverages: A review, *J. Funct. Foods.* 4 (2012) 53–65, <https://doi.org/10.1016/J.JFF.2012.01.002>.
- [44] T.L.S. Silva, S. Morales-Torres, J.L. Figueiredo, A.M.T. Silva, Multi-walled carbon nanotube/PVDF blended membranes with sponge-and finger-like pores for direct contact membrane distillation, *Desalination.* 357 (2014) 233–245, <https://doi.org/10.1016/j.desal.2014.11.025>.